Chemical Engineering Journal 148 (2009) 312–318

Contents lists available at ScienceDirect

Chemical Engineering Journal

journal homepage: www.elsevier.com/locate/cej

Distribution of HCN, NH_3, NO and N_2 in an entrained flow gasifier

Chen Zhong, Yuan Shuai, Liang Qinfeng, Wang Fuchen*, Yu Zunhong

Ministry of Education Key Laboratory of Coal Gasification, East China University of Science and Technology, Mei Long Road No.130, Shanghai 200237, PR China

ARTICLE INFO

Article history:
Received 4 May 2008
Received in revised form 28 August 2008
Accepted 29 August 2008

Keywords:
HCN
NH_3
NO
N_2
Entrained flow gasifier
Coal water slurry

ABSTRACT

A laboratory gasifier with the opposed multi-burners (OMB) was used to investigate the formation of nitrogen compounds during coal water slurry (CWS) gasification. Various axial and radial concentrations of HCN, NH_3, NO and N_2 (nitrogen compounds) in the gasifier were measured. The concentrations of HCN, NH_3 and NO (nitrogen pollutants) were maximal at the nozzle plane and decreased along the axial distances. Moreover, the ordering of nitrogen compounds in exit was N_2 > HCN > NH_3 > NO. An increase in O_2/C ratio tends to favour the formation of N_2. Flow field distribution resulted in the radial concentrations uniform at the exit and low near the side-wall at other axial positions. The results showed the majority of nitrogen pollutants formed from coal volatile nitrogen during the rapid devolatilization. HCN and NH_3 formed mainly from devolatilization at the nozzle plane but were not thoroughly converted from the reduction of NO. H_2O in CWS played a vital role in converting coal-N into NH_3 and HCN by providing H.

© 2009 Published by Elsevier B.V.

1. Introduction

Coal water slurry (CWS) gasification technology has prominent advantages over other gasification processes, including its safety, controllability, capability of utilizing nearly any types of coals and almost complete carbon conversion. It has been widely used in chemical production and power generation. During gasification production, coal-N mainly forms HCN, NH_3, N_2 and NO, which has many negative effects on environment, safe stability and long run of industrial system. In scrubbing and purging process, some NH_3 and HCN remaining in syngas would be the precursors of NO_x in integrated gasification combined cycle (IGCC). In methanol scrub section, NH_3 lowers desulphurization efficiency, and causes dehydrogenation catalysts poisoning in urea synthetic section. NH_3 dissolved in scrubbing leads to the increase of pH value of circulating water, and decayed the effect of stabilizer in circulating water. NH_4HCO_3 and $CaCO_3$ are easily crystallized in low temperature sections, resulting in equipment abrasion and pipeline plugging. Therefore, large quantities of circulating water need to be discharged and great quantities of fresh makeup-water must be supplied. The regenerative cycle is energy-consumptive and the treatment methods are not yet fully developed.

Due to problems mentioned above, it is desirable to understand the formation processes of nitrogen compounds during gasification in an attempt to minimize them by pollution control in production. This aims to develop low-emission gasification-based technologies for power generation or for the production of liquid fuels and chemicals.

There have been many significant studies examining coal-N conversion during gasification in fixed bed and fluidized-bed gasifier [1–4]. Studies in entrained-flow gasifier were rarely reported. Price et al. measured the distribution of pollutants in a laboratory gasifier [5]. Hansen et al. measured nitrogen compounds in effluents from an entrained coal gasifier [6]. Highsmith et al. investigate the fate of nitrogen and sulphur pollutants in a laboratory-scale entrained flow gasifier [7]. However, the conversion mechanism of CWS nitrogen in entrained flow gasifier was unknown. The purpose of this study was to investigate the mechanisms for the formation of nitrogen compounds during entrained flow gasification of CWS in oxygen (99.6%). Based on the successful application of OMB CWS gasification technology [8,9], a laboratory-scale OMB gasifier, simulating as near as practicable the conditions expected in a full-scale OMB gasifier, was constructed for the investigation.

2. Experimental

2.1. Coal water slurry sample

One CWS produced by Bayi Coal Water Slurry plant was selected for use in this study and its properties are presented in Table 1.

2.2. Gasifier

Fig. 1 shows the sketch of the gasifer used in this study. The gasifier mainly consisted of a gasifier chamber flanged by five sections and a quench bath. Each section contained thermocouples

* Corresponding author. Tel.: +86 21 64250784; fax: +86 21 64251312.
E-mail address: wfch@ecust.edu.cn (F. Wang).

1385-8947/$ – see front matter © 2009 Published by Elsevier B.V.
doi:10.1016/j.cej.2008.08.038

Table 1
Coal water slurry sample properties.

Concentration (%)	Viscosity (mPa s)	P_{cwm}, +0.3 mm (%)	P_d, −0.075 mm (%)	Proximate analysis (wt.%)				Ultimate analysis (wt.%)					$Q_{net,v,cws}$ (MJ/kg)	Ash fusion/point (°C)
				M_{ar}[1]	A_{ar}	V_{ar}	FC_{ar}	C_{ar}	HC_{ar}	N_{ar}	S_{ar}	O_{ar}[2]		
67.2	1215	0.08	81.87	32.8	6.90	22.07	38.23	49.68	2.84	0.95	0.43	6.4	19.30	1330

[1]as received basis; [2]by difference.

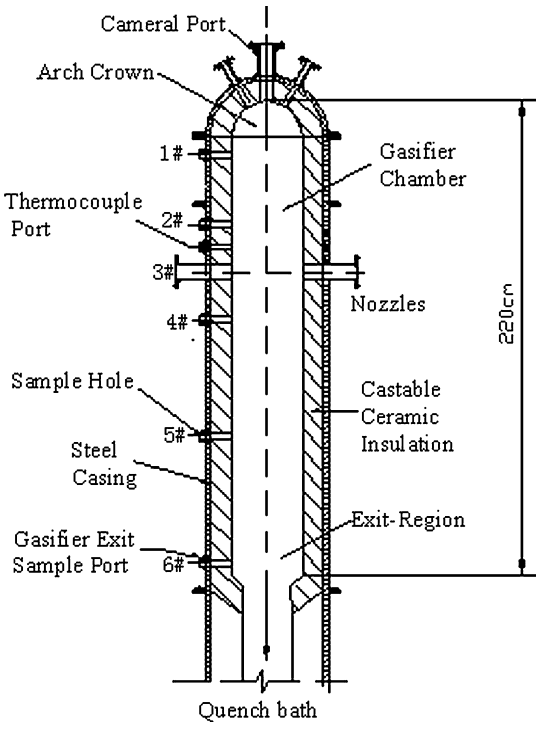

Fig. 1. Schematic of the gasification reactor.

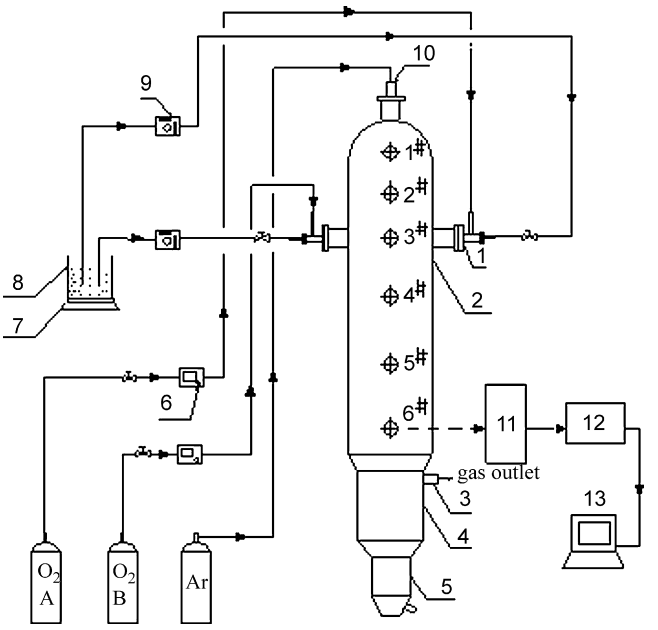

Fig. 3. Flow sheet of experiment. (1) Nozzle; (2) gasification furnace; (3) synthetic gas vent; (4) cleaning and cooling room; (5) slag chamber; (6) mass flowmeter; (7) electronic balance; (8) fuel storage tank; (9) gear pump; (10) video camera; (11) gas treating cabinet; (12) gas chromatography or mass spectrometer; (13) computer

and sample probes. The nominal inner diameter was 30 cm and the height of gasifier chamber was 220 cm. The outmost layer was stainless-steel casing. Castable ceramic insulation (wall thickness 20 mm) lined the interior of each section. On the top of the reactor, a video camera protected by argon was equipped to oversight the inner case. The gasifer featured four diametrically opposed burners in the side-wall at the upper part, and the included angle between any adjacent two burners is 90°. Fig. 2 shows the schematic

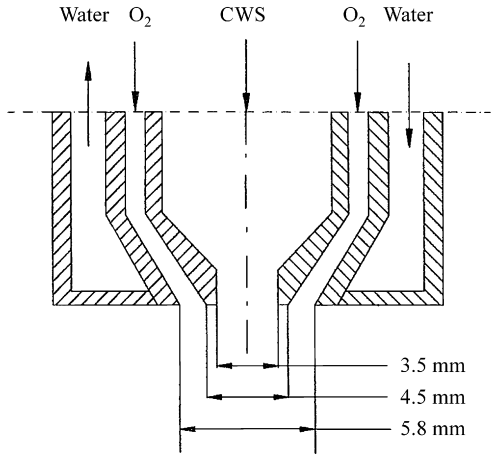

Fig. 2. Schematic of nozzle.

of nozzle. Oxygen from high-pressure gas cylinders flowed into the nozzle's outer channel. Control valves were used to stabilize flow and avoid pressure oscillations. CWS was continuously fed into the nozzle's inner channel by single-screw pumps. Opposed turbulent flow fields were obtained by four opposed round nozzles.

Four streams of fuel and oxygen were injected through, atomized and impinged at the nozzle plane to form impinging flow field inside the gasifier. Thus rapid pyrolysis and gasification occurred immediately under much high temperature. From the gasification chamber, the raw syngas flowed into quench chamber to be scrubbed, cooled and then discharged.

2.3. Operating conditions

Gasification experiments were carried out with gasifying agent O_2 (99.6 vol.%) at atmospheric pressure. Diesel oil was combusted to preheat the gasifier for about 4 h before CWS was fed in. When the gasification temperature was almost invariable, measurements began and usually took about 3 h.

The effects of O_2/C ratio on the distribution of nitrogen compounds were observed. The O_2/C ratio was varied from 0.6 to 1.4 Nm^3/kg. The radial sampling points in each axial position (distance from the centerline to the wall) were 0, 4, 8, 11 and 15 cm. The nozzle plane (3#) was marked as 0 cm. The upper (1# and 2#) and down (4#, 5# and 6#) were marked as negative and positive value, respectively. The axial sampling points (distance from the nozzle plane) were denoted in Fig. 3 and Table 2.

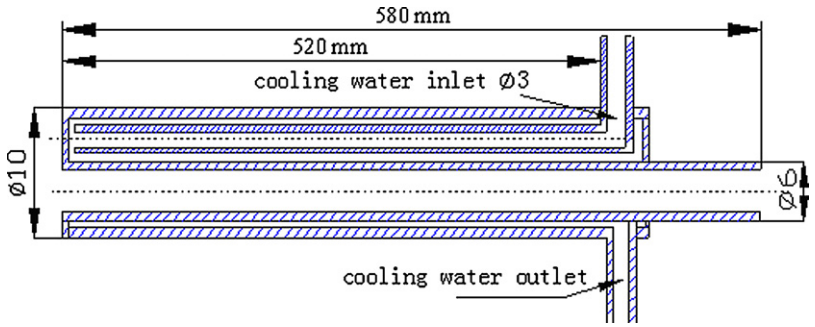

Fig. 4. Schematic of sample probe.

Table 2
Distance between sample position and nozzle plane.

Location number	Axial position (cm)
1#	−50
2#	−20
3#	0
4#	20
5#	96
6#	144

2.4. Sampling and analysis

Sample probe with water jacketed was made of 316 stainless-steel 6 mm i.d. (Fig. 4). Water was injected into the sampling area from small injection port to the tip of probe to cool the gas from the reactor. In measuring, sampling probes were horizontally inserted into the gasifier and could be traversed radially across the reactor from the centerline to the wall (Fig. 5).

HCN or NH_3 was analyzed with HCN or NH_3 Gas Detection Tube which could detect them to a ppm level. The tubes contain certain reagents which could react with the specific gas species to be measured. As the gas sample was pulled through the tube by a specific pump, a length of the tube was discolored in proportion to the HCN or NH_3 concentration. NO was measured with flue gas analyzer. N_2 was measured online by gas chromatography. The analysis methods are summarized in Table 3.

3. Results and discussion

3.1. Effect of flow field on concentration distribution

The distribution of nitrogen compounds was shown in Fig. 6. In all cases, the concentrations of HCN, NH_3 and NO appeared maximal at the nozzle plane and decreased dramatically along the axial distances. The release processes of coal-N in entrained flow gasification are closely correlated with flow field and can be classified into primary reactions and secondary reactions. Which type of reaction occurs in one area of the gasifier depends on the flow characteristic and mixing process. A structure of flow field was formed when four strands of jet stream were ejected and impinged, which might be described as Fig. 7 [8].

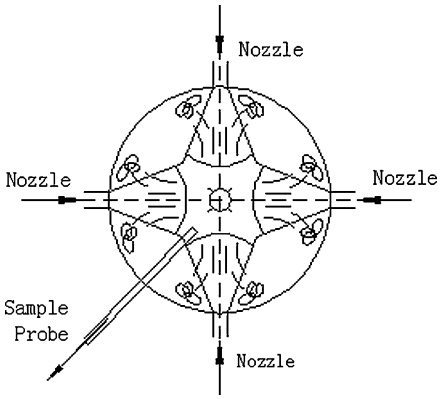

Fig. 5. Schematic plan of sampling method at nozzle plane.

Jet flow region (I): flow ejected from the burners with high velocity entrains materials from the neighboring area into the jet downstream. The width of the jet flow is increased and the velocity is decreased. Finally, the boundary of the jet flow from one burner intersects with the boundaries of the jet flows from neighboring burners.

Impinging region (II): impinging region is formulated where boundaries of jet flows intersect. At the center of the impinging region, turbulent impinging is generated. The velocity direction of the flow is deflected from the jet axis direction to the gasifier axis direction under the effect of impinging. In this region, velocity fluctuation is strenuous, turbulent flow has high strength and mixing effect is well.

Impinging stream flow region (III): after jet flow impinging, the directions of the main streams are changed to the gasifier axial direction. The impinging flow streams are formed above/beneath the impinging region with similar flow characteristics but in different directions. Impinging streams, like jet flows, can entrain fluid from the neighboring area too, which increases the width of the

Table 3
Summary of analysis methods.

Component	Phase	Analysis method	Precision or detection limits
HCN	Gas	HCN detection tube	<±5%, 1 ppm
NH_3	Gas	NH_3 detection tube	<±5%, 1 ppm
NO	Gas	Flue gas analyzer	<±5%, 1 ppm
N_2	Gas	Gas chromatography	2500 mv × ml/mg
CO, H_2, CO_2, CH_4, Ar	Gas	Mass spectrometer	1 ppm

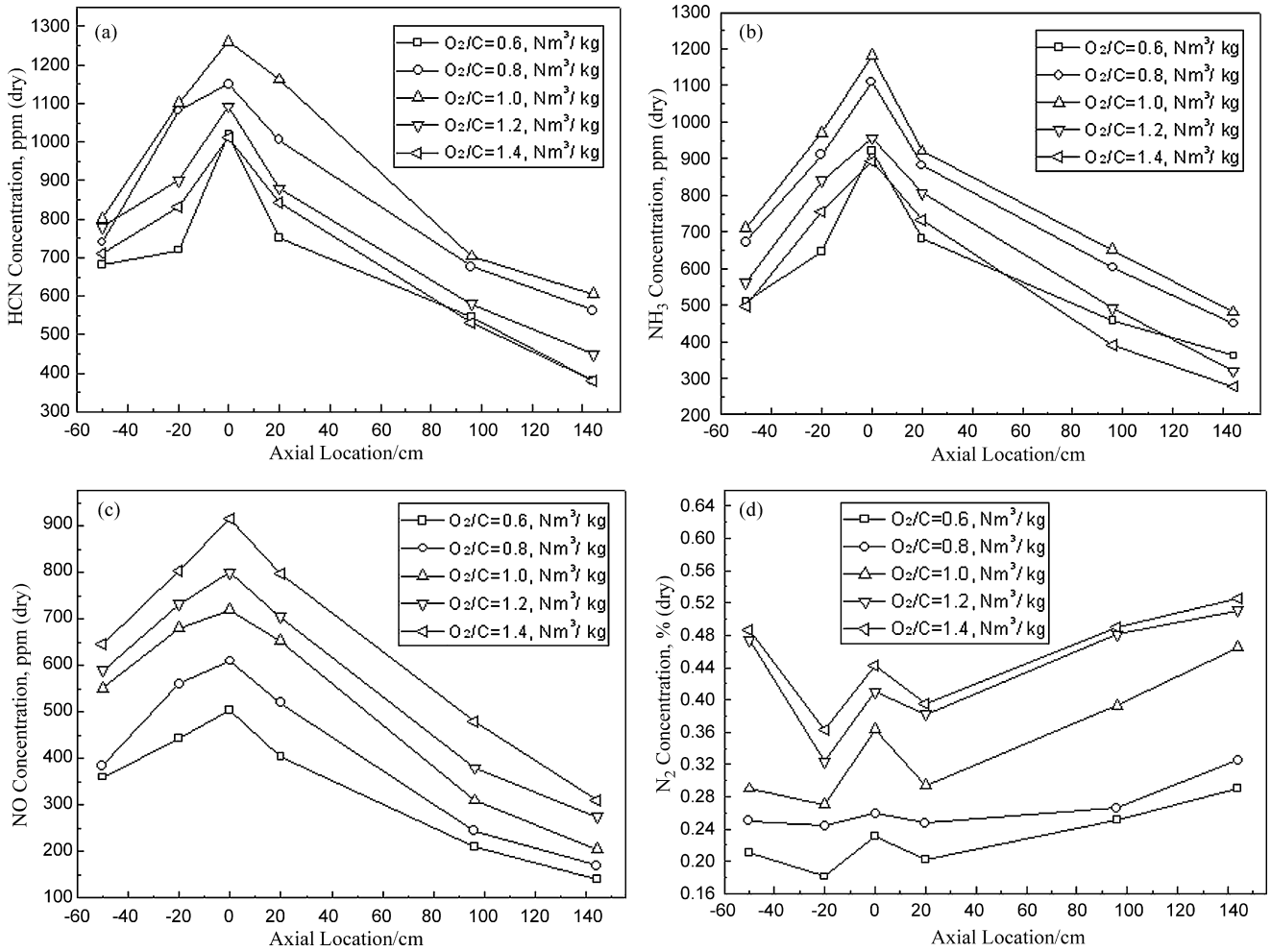

Fig. 6. Axial concentrations of HCN (a), NH_3 (b), NO (c) and N_2 (d).

impinging streams and decrease the axial velocity of impinging streams.

Recirculation region (IV): since jet flows and impinging streams can entrain the fluid of the neighboring area, recirculation phenomena exists at the near edge of the jet flow region and the impinging stream flow region.

Reentry flow region (V): part of the fluid from the upward impinging stream region impinges to the top of the gasifier and reenters downward along the wall.

Plug flow region (VI): at the bottom of the OMB gasifier, the velocity main direction is downward. At any part of the cross-section of the gasifier vertical to its axis, the velocity is almost identical in magnitude. The flow can be recognized as plug flow.

CWS gasification is a complicated physicochemical reaction process, which includes the atomization of CWS, rapid heating, evaporation of water, devolatilization, carbon gasification and inter-reactions. Coal-N existed mainly in the form of aromatic nitrogen [10–12]. Heavy hydrocarbons, aromatic compounds and the majority of volatile nitrogen (volatile-N) were liberated simultaneously from coal particles in devolatilization [13]. Coal-N primary reactions include the release of volatile-N and the break of nitrogen heterocyclic ring, in which abundance of CN and N were liberated and then combined instantly with H and O, forming large amounts of HCN, NH_3 and NO at the nozzle plane (Fig. 6(a–c)). This is the first stage which transfers solid aromatic nitrogen into gaseous nitrogen pollutants. Primary reaction process determines the initial concentrations of nitrogen pollutants. Therefore, nitrogen pollutants mainly come from volatile-N in the rapid heating process of coal particles. Primary reaction regions include jet stream region (I) and impinging region (II), which are near the feeding point. The following reaction processes may be considered:

$$\text{Coal-N} \rightarrow \begin{cases} \text{Volatile-N} \rightarrow \text{HCN},\ \text{NH}_3,\ \text{NO} \\ \text{Char-N} \end{cases} \quad (1)$$

Reaction (1) is primitive reaction, which is greatly faster than the micro-mixing process [14]. Thus, the maximum of HCN, NH_3 and NO were immediately reached near the feeding point, i.e. at the nozzle plane.

Coal-N secondary reactions include: (1) inter-conversion reactions of nitrogen pollutants; (2) homogeneous and heterogeneous reactions in which nitrogen pollutants react with permanent gases (e.g. H_2, CO, CH_4, H_2O) and chars; (3) heterogeneous reactions in which residual char-N react with the gaseous to convert some char-N to gaseous nitrogen compounds. The reactions in impinging stream region (III) belong to secondary reactions. Coal pyrolysis and devolatilization generated large quantities of chars which mingled with some unreleased char-N. Along with the char gasification, char-N continuously released, forming gaseous nitrogen compounds. This process was in direct ratio of carbon release rate and was much slower and minor than the releasing and cracking process of volatile-N [15]. Char-N released got the same conversion

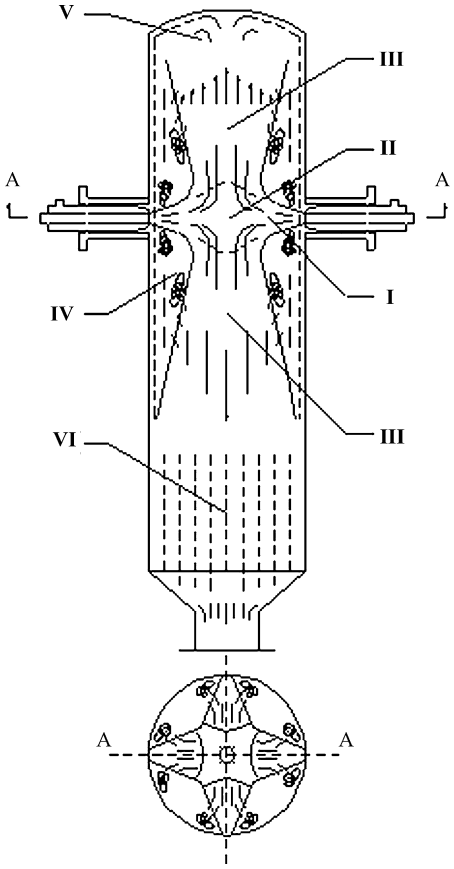

Fig. 7. Diagram of flow field in OMB gasifier. (I) Jet flow region; (II) impinging region; (III) impinging stream flow region; (IV) recirculation region; (V) reentry flow region; (VI) plug flow region

reactions of volatile-N. In region (III), products of primary reaction continue the subsequent secondary reactions and the conversion processes were probably described as (2)–(4).

$$NO \xrightarrow[Char]{C_xH_y,\ H,\ CO} N_2,\ HCN,\ NH_3 \quad (2)$$

$$NO \xrightarrow{NH_i,\ HCN} N_2 \quad (3)$$

$$\text{Char-N} \rightarrow N_2,\ HCN,\ NH_3 \quad (4)$$

Most reactions of (2) and (3) were homogeneous reactions and it was reasonable to consider their reaction rates were greatly faster than these in (4) [8,14,16–18]. In the secondary reaction regions, nitrogen pollutant conversion reactions happened in the similar types of (2) and (3). Therefore, as the distance from nozzle plane increased, nitrogen pollutants reduced and the majority of them converted to N_2. Fig. 6 proves these results.

3.2. Effect of O_2/C ratio on axial concentration of nitrogen compounds

The relationship between the ratio of O_2/C and the corresponding nozzle plane temperature is listed in Table 4. The temperatures were tested by thermal couples near the wall of nozzle plane.

Fig. 6 shows axial concentrations in different O_2/C ratios. Results are reported as arithmetic mean values from the five radial locations. The effects of O_2/C ratios on the mean concentrations of HCN, NH_3, NO and N_2 are illustrated.

Table 4
Relationship of O_2/C and nozzle plane temperature.

O_2/C (Nm^3/kg)	Nozzle plane temperature (°C)
0.6	1247
0.8	1361
1.0	1469
1.2	1550
1.4	1657

From Fig. 6(a) and (b), the highest concentrations of HCN and NH_3 appeared at the O_2/C ratio of 1.0, while NO concentration increased in all axial locations with the increase of O_2/C ratio. Percents of devolatilized nitrogen depend on the heating environment of coal particles and increase with the raise of gasification temperature [15]. At the lowest O_2/C ratio of 0.6, the CWS nebulization appeared to be bad and the gasification temperature was low, resulting in the decrease of heating rate of coal particles. As a result, the volatile-N devolatilized and cracked were small. With the raise of O_2/C ratio, the gasifier temperature increased and the release of volatile-N increased. The raise O_2/C ratios tend to favour the formation of NO at the nozzle plane (Fig. 6(c)). NO was difficult to reduce in the richer oxygen atmosphere, and HCN and NH_3 could be partly oxidized. In spite of the fuel-rich environment, high NO levels still appeared in the exit. This may be due to the short residence time which is insufficient for complete reduction of NO.

From Fig. 6(a) and (b), HCN was about 100–200 ppm higher than that of NH_3 at the same O_2/C ratio and axial location. This might be broadly illustrated that when aromatic nitrogen broke, CN active group was dominated. Formation of NH_3 needed more H and was a relatively slow process, while formation of HCN was much easier. NH_3 was more decomposable than HCN, which may be another reason [12,13].

As the raise of O_2/C ratio, the N_2 concentrations at the same position increased (Fig. 6(d)), which indicates that oxygen-rich atmosphere is favourable for the formation of N_2. Different from the trends of nitrogen pollutants, N_2 concentration decreased slightly and then increased significantly as the distances from the nozzle plane increased. In the effluent, N_2 was the major nitrogen product and its concentration was greatly higher than that at the nozzle plane. These observations provide the following insight: some percent of N_2 in gasifying agent (N_2 about 0.4 vol.%) were cracked ($N{\equiv}N \rightarrow N + N$) and took part in the formation of nitrogen pollutants near the nozzle plane. If all N_2 in gasifying agent could crack to N and took part in gasification, the ratio of N in N_2 to coal-N was at most 26.2%. The data in Fig. 6 show the increased N_2 with the decrease of the other nitrogen compounds, implying that significant quantities of N_2 came from inter-conversion reactions of nitrogen pollutants. But the totally decreased amount of N element in nitrogen pollutants were slightly lower than the increased amount of N in N_2, suggesting that some of N_2 came from char-N.

3.3. Radial concentration profiles for nitrogen pollutants

Fig. 8 illustrates the radial profile data for HCN, NH_3 and NO in the O_2/C ratio of 1.0 Nm^3/kg. This ratio was selected because maximal pollutant level was achieved under this condition. Significant variations in nitrogen pollutant concentrations were observed with both radial and axial locations, especially near the regions of the nozzle plane (1#, 2# and 4#). Toward the exit-regions (5# and 6#), radial concentration profiles for pollutants were more uniform and the minimal axial concentrations of HCN, NH_3 and NO appeared. Similar trends were obtained in other O_2/C ratios.

Entrainment phenomena and turbulent diffusion of jet stream generate large range of reflux region among the reactor wall, jet

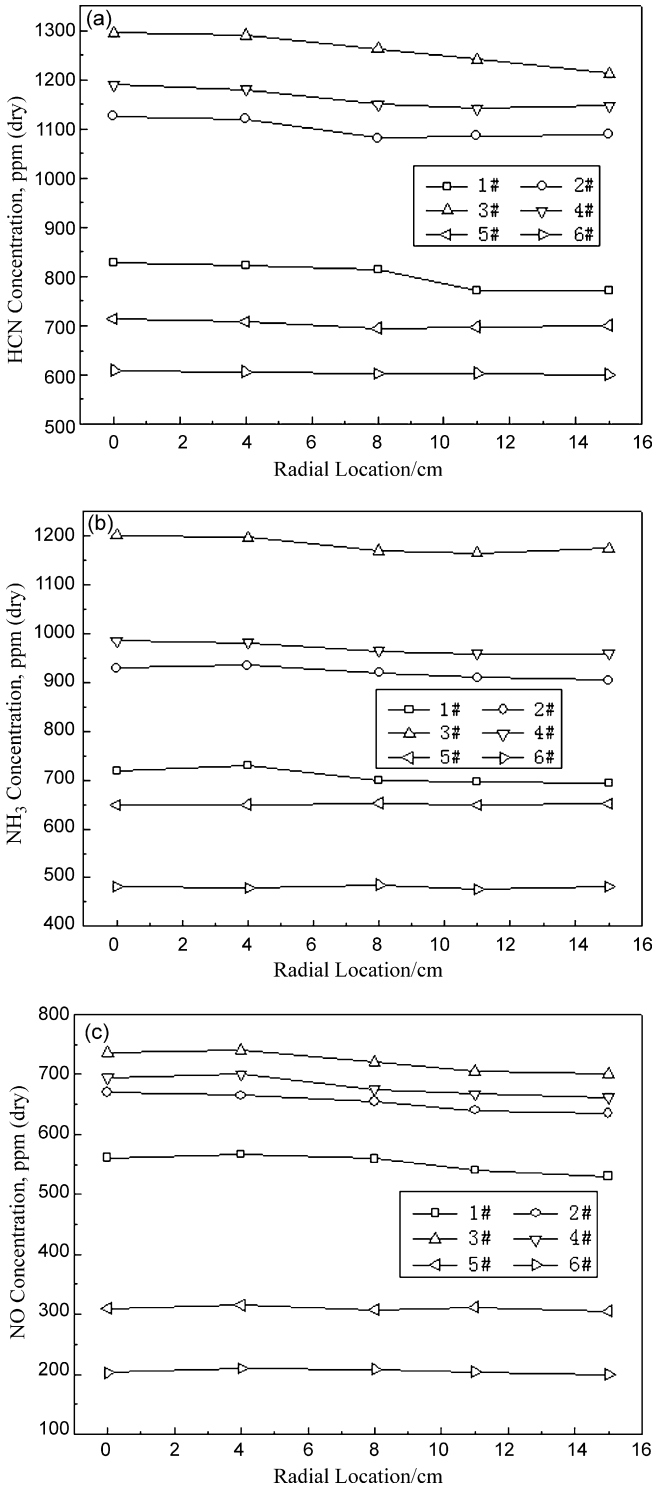

Fig. 8. Radial concentration profiles of HCN (a), NH_3 (b) and NO (c).

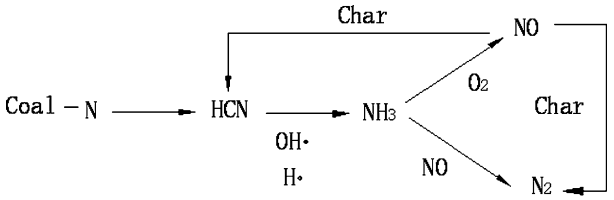

Fig. 9. Conversion mechanism of coal nitrogen from literature.

stream and impinging stream region [19]. Near the top arch crown (1# region), the reentry flow regions (V) were formed. Secondary reactions were absolutely dominant in the reflux flow (IV) and reentry flow (V) regions, where reactants and products recirculate. Because of high level of entrainment and turbulent diffusion, residence time in the above two regions is longer than that in other regions, which have greater influence on nitrogen conversion. Thus, the secondary reactions were more complete in regions (IV) and (V) than those in (III), which resulted in decrease of nitrogen pollutants near the side-wall. Fig. 8 shows this radial trend.

Toward the exit of gasifier chamber, velocity directions were mainly downward and the homogeneous plug flow region formed, in which secondary reactions were still happening and radial concentration profiles were almost uniform.

3.4. Effect of steam on nitrogen pollutant concentrations

Studies have reported that H is very critical for the formation of NH_3 and HCN [3,4]. The presence of H_2O in CWS (32.8%) leads to high concentrations of HCN and NH_3. H_2O has the following effects: (1) H_2O supplies much H to combine with CN and N. (2) H attack nitrogen aromatics and make them activated and broken to liberate much more CN and N. (3) H_2O results in fuel-rich atmosphere and more NO reduction.

3.5. Nitrogen pollutant conversion mechanism

Fig. 9 gives a different mechanism postulated by Haynes [20] and Smith et al. [21]. They reported that HCN is formed early, directly from devolatilization. However, the presence of OH and H convert HCN to NH_3, and then NH_3 is oxidized to NO and N_2. In the oxygen lean zone, NO inter-reacts with char and is converted back to HCN, NH_3 and N_2. Two major routes in Fig. 9 may be described as the following reactions:

$$HCN + H_2O = NH_3 + CO \quad (5)$$

$$NH_3 + (5/2)O_2 = NO + (3/2)H_2O \quad (6)$$

The chemical equilibrium constants of (5) and (6) in 1573 K are $K_1 = 28.24$ and $K_2 = 5.96 \times 10^{-6}$, respectively. These low constants may indicate the two conversion routes to be difficult.

Fig. 10 is a postulated mechanism model proposed from the experimental data. Due to the high temperature in entrained flow gasifier, volatile-N (aromatic nitrogen) were liberated from coal particles in rapid devolatilization and cracked instantly to CN and N,

Table 5
Comparison of different experiments.

Authors	Feed nozzle	O_2/C	Steam/coal	Pressure (atm)	C%	H%	N%	Effluent concentrations		
								HCN (ppm)	NH_3 (ppm)	NO (ppm)
Tracy D. Price	Top of the reactor	1.07	0.24	1	77.6	1.6	0.6	1470	1000	500
John R. Highsmith	Top of the reactor	1.26	0.27	1	72.0	1.4	0.6	1570	1422	347
Present work	Opposed four nozzle	1.0	–	1	49.7	2.84	0.95	605	481	205

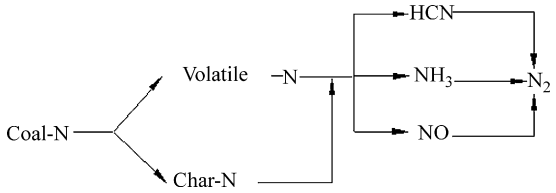

Fig. 10. Conversion mechanism of coal nitrogen based on present work.

forming HCN, NH_3 and NO. The majority of HCN, NH_3 and NO were formed early, directly and simultaneously from coal devolatilization. Homogeneous and heterogeneous conversion reactions led to HCN, NH_3 and NO decayed and most of them were converted to N_2. Compared with Fig. 9, Fig. 10 fits more this laboratory results.

3.6. Comparison with other gasifiers

Results reported by other researchers are compared in Table 5. Tracy D. Price et al. and John R. Highsmith et al. have found that high concentrations of HCN, NH_3 and NO occurred in the exit of gasifier [5,7], however, in our own work the effluent nitrogen pollutants were slightly low, although H_2O in CWS tend to favour the formation of HCN and NH_3. This may be due to the difference in flow field distribution between OMB gasifier and other gasifiers [5,8,22]. OMB gasifier had a longer residence time (about 1.5–2.0 s) than other gasifiers (about 400 ms), which enables secondary reactions to proceed more completely. Therefore, large numbers of HCN, NH_3 and NO could convert to N_2.

4. Conclusions

(1) Most amounts of HCN, NH_3 and NO came from the release of volatile-N in the rapid heating process of coal particles. Nitrogen pollutants were initially produced and reached maximum at the nozzle plane and the ordering was HCN > NH_3 > NO. The formation of HCN is easier and more direct than NH_3.
(2) HCN and NH_3 formed early, directly from devolatilization but not thoroughly from the reduction of NO. Most of nitrogen pollutants were decayed and converted to N_2 and the raise of O_2/C tends to favour the formation of N_2.
(3) Part of N_2 in gasifying agent cracked and took part in the formation of nitrogen pollutants near the nozzle plane.
(4) Flow field affected the coal-N conversion processes and the distribution of HCN, NH_3, NO and N_2.
(5) H_2O in CWS played a vital role in converting coal-N into HCN and NH_3 by providing H.

Acknowledgements

This work was financially supported by National Basic Research Program of China (No. 2004CB217703) and Program for Changjiang Scholars and Innovative Research Team in University (IRT0620). The authors also acknowledge Prof. Wang Jie (School of Resource and Environmental Engineering, ECUST) for his helpful suggestions.

References

[1] T. Hasegawa, M. Sato, Study of ammonia removal from coal-gasified fuel, Combust. Flame 114 (1998) 246–258.
[2] J. Leppälahti, Formation of NH_3 and HCN in slow-heating-rate inert pyrolysis of peat, coal and bark, Fuel 74 (1995) 1363–1368.
[3] L.P. Chang, K.C. Xie, C.Z. Li, Release of fuel-nitrogen during the gasification of Shenmu coal in O_2, Fuel Process. Technol. 85 (2004) 1053–1063.
[4] L.J. McKenzie, F.J. Tian, X. Guo, C.Z. Li, NH_3 and HCN formation during the gasification of three rank-ordered coals in steam and oxygen, Fuel 87 (2008) 1102–1107.
[5] T.D. Price, L.D. Smoot, P.O. Hedman, Measurement of nitrogen and sulfur pollutants in an entrained-coal gasifier, Ind. Eng. Chem. Fundam. 22 (1983) 110–116.
[6] L.D. Hansen, L.R. Phillips, N.F. Mangelson, M.L. Lee, Analytical study of the effluents from a high-temperature entrained flow gasifier, Fuel 59 (1980) 323–330.
[7] J.R. Highsmith, N.R. Soelberg, P.O. Hedman, L.D. Smoot, A.U. Blackham, Entrained flow gasification of coal. 2. Fate of nitrogen and sulphur pollutants as assessed from local measurements, Fuel 64 (1985) 782–788.
[8] F.C. Wang, Z.J. Zhou, Z.H. Dai, X. Gong, G.S. Yu, Q.F. Liang, H.F. Liu, Y.F. Wang, Z.H. Yu, Development and demonstration plant operation of an opposed multi-burner coal–water slurry gasification technology, Front Energ. Power Eng. China 3 (2007) 251–258.
[9] Key Laboratory of Coal Gasification of Ministry Education, http://icct.ecust.edu.cn/en/app/app.htm, 2005.
[10] S.M. Kirtley, O.C. Mullins, J. van Elp, S.P. Cramer, Nitrogen chemical structure in petroleum asphaltene and coal by X-ray absorption spectroscopy, Fuel 72 (1993) 133–135.
[11] K.D. Bartle, D.L. Perry, S. Wallace, The functionality of nitrogen in coal and derived liquids: an XPS study, Fuel Process. Technol. 15 (1986) 351–361.
[12] L.P. Chang, The study on the formation and release process of nitrogen compounds during the coal pyrolysis and gasification, Ph.D. Thesis, Taiyuan University of Technology, China, 2004.
[13] L.D. Smoot, D.T. Pratt, Pulverized-Coal Combustion and Gasification, Tsinghua Press, 1992, pp. 283.
[14] A.E. Axworthy, G.R. Schneider, M.D. Shuman, V.H. Dayan, Chemistry of fuel nitrogen conversion to nitrogen oxides in combustion, Washington, DC, US Environmental Protection Agency, EPA-600/2-76-039, 1976.
[15] L.D. Smoot, P.J. Smith, Coal Combustion and Gasification, A Division of Plenum Publishing Corporation, 1985, pp. 86.
[16] E.G. Masdin, R.H. Essenhigh, Burning times of liquid fuel drops in a convection radiation field, Combust. Flame 2 (1958) 443–446.
[17] M.W. Thring, M.P. Newby, Combustion length of enclosed turbulent jet flames, Sym. (Int.) Combust. 4 (1953) 789–796.
[18] X.X. Sun, J.Y. Chen, Physical Chemistry Foundation of Coal Powder Combustion, HUST Press, 1991, pp. 185.
[19] Z.H. Yu, C.D. Shen, F.C. Wang, K.J. Xiao, X. Gong, Process analysis and 3-region model for residual oil gasifier, Acta Petrol. Sin. 3 (1993) 61–68.
[20] B.S. Haynes, Reactions of ammonia and nitric oxide in the burnt gases of fuel-rich hydrocarbon–air flames, Combust. Flame 28 (1977) 81–91.
[21] P.J. Smith, S.C. Hill, L.D. Smoot, Theory for NO formation in turbulent coal flames, Sym. (Int.) Combust. (1982) 1263–1270.
[22] J.L. Xu, Z.H. Dai, Q.H. Li, W.F. Li, H.F. Liu, F.C. Wang, Z.H. Yu, Particle residence time distribution in entrained-flow gasifier, J. Chem. Ind. Eng. (China) 59 (2008) 53–57.